Membrane-Induced Secondary Structures of Neuropeptides: A Comparison of the Solution Conformations Adopted by Agonists and Antagonists of the Mammalian Tachykinin NK_1 Receptor†

Tracy L. Whitehead,‡ Sharon D. McNair,‡ Chad E. Hadden,§ John K. Young,|| and Rickey P. Hicks*,‡

Department of Chemistry, Mississippi State University, Mailstop 9573, Mississippi State, Mississippi 39762, Pharmaceutical Development, Rapid Structure Characterization Group, Pharmacia & Upjohn, Kalamazoo, Michigan 49001-0199, and Department of Chemistry, Colgate University, 13 Oak Drive, Hampton, New York 13346

Received November 19, 1997

We present what we believe to be the first documented example of an inducement of distinctly different secondary structure types onto agonists and antagonists selective for the same G-coupled protein receptor using the same membrane-model matrix wherein the induced structures are consistent with those suggested to be biologically active by extensive analogue studies and conventional binding assays. ^{1}H NMR chemical shift assignments for the mammalian NK_1 receptor-selective agonists α-neurokinin (NKA) and β-neurokinin (NKB) as well as the mammalian NK_1 receptor-selective antagonists [D-Pro^2,D-Phe^7,D-Trp^9]SP and [D-Arg^1,D-Pro^2,D-Phe^7,D-His^9]SP have been determined at 600 MHz in sodium dodecyl sulfate (SDS) micelles. The SDS micelle system simulates the membrane−interface environment the peptide experiences when in the proximity of the membrane-embedded receptor, allowing for conformational studies that are a rough approximation of in vivo conditions. Two-dimensional NMR techniques were used to assign proton resonances, and interproton distances were estimated from the observed nuclear Overhauser effects (NOEs). The experimental distances were used as constraints in a molecular dynamics and simulated annealing protocol using the modeling package DISCOVER to generate three-dimensional structures of the two agonists and two antagonists when present in a membrane-model environment to determine possible prebinding ligand conformations. It was determined that (1) NKA is helical from residues 6 to 9, with an extended N-terminus; (2) NKB is helical from residues 4 to 10, with an extended N-terminus; (3) [D-Pro^2,D-Phe^7,D-Trp^9]SP has poorly defined helical properties in the midregion and a β-turn structure in the C-terminus (residues 6−9); and (4) [D-Arg^1,D-Pro^2,D-Phe^7,D-His^9]SP has a helical structure in the midregion (residues 4−6) and a well-defined β-turn structure in the C-terminus (residues 6−10). Attempts have been made to correlate the observed conformational differences between the agonists and antagonists to their binding potencies and biological activity.

Introduction

The tachykinins, a family of evolutionarily conserved neuropeptides which have been shown to exhibit a vast range of physiological activities that are cardiovascular, respiratory, and gastrointestinal in nature, exist in a variety of biological species.[1] Their presence has been implicated in a number of physiological and neurological diseases, most notably Crohn's, Alzheimer's, and Parkinson's diseases.[2] Due to the potential for drug development, the conformational analysis of the tachykinins and their analogues has received a great deal of attention over the past decade in the hopes that insight concerning the possible biologically active conformations for the ligands and the development of a structure−activity relationship between the ligands and their receptors may be obtained.

The earliest known members of the tachykinin family are those that are present in mammalian systems. Currently, there are five known mammalian tachykinins: substance P (SP),[3,4] α-neurokinin (NKA), β-neurokinin (NKB),[5−7] neuropeptide K (NPK),[8] and neuropeptide γ (NPγ).[9] All five peptides possess a common C-terminal pentapeptide sequence: Phe-(X)-Gly-Leu-Met-NH_2, where (X) = Phe in the case of substance P and (X) = Val for NKA, NKB, NPK, and NPγ. This common region, often referred to as the "message" portion of the peptide, is believed to be responsible for receptor activation upon binding.[10]

The N-terminal sequence or "address" region of the peptide varies to a certain extent in all five mammalian tachykinins. It is this variation in length and amino acid composition which is believed to play a role in determining the selectivity of each neuropeptide for a particular receptor subtype,[10] with SP, NKA, and NKB

† Abbreviations: SP, substance P; NKA, α-neurokinin; NKB, β-neurokinin; NK_1, neurokinin 1; NPK, neuropeptide K; NPγ, neuropeptide γ; SDS, sodium dodecyl sulfate; 2D, two-dimensional; NMR, nuclear magnetic resonance; WATERGATE, water suppression by gradient-tailored excitation; TOCSY, total correlated spectroscopy; NOESY, nuclear Overhauser enhancement spectroscopy; NOE, nuclear Overhauser effect; rmsd, root-mean-square deviation; TFE, 2,2,2-trifluoroethanol; MD, molecular dynamics; SA, simulated annealing.

* To whom correspondence should be addressed. Tel: (601)-325-3584. Fax: (601)-325-1618. E-mail: rph1@ra.msstate.edu.
‡ Mississippi State University.
§ Pharmacia & Upjohn.
|| Colgate University.

S0022-2623(97)00789-9 CCC: $15.00
Published on Web 04/08/1998

being the primary endogenous ligands for the NK_1, NK_2, and NK_3 G-protein-coupled receptors, respectively.[11] Although selectivity occurs primarily in the order given, there is a certain degree of cross-reactivity which occurs for the three peptides among the three membrane-embedded receptor subclasses.[12,13] This cross-reactivity suggests that the tachykinin agonists may adopt a similar bioactive conformation (the conformation associated with receptor recognition, binding, and activation) that is recognized by the NK_1 receptor.

Such an idea of a message−address model for the tachykinins and their receptors has existed for some time but fails to illustrate one very important aspect of ligand−receptor interactions: the conformation factor. The assumption that ligands are selective for receptors based solely upon their primary sequence is oversimplified, ignoring vital aspects of ligand−receptor binding such as steric hindrance, side-chain orientation, and thermodynamically driven peptide folding, all of which are known to play a major role in the ability of a ligand to bind to its receptor.[14] Therefore, to gain a better understanding of the process of ligand−receptor recognition and binding, one must incorporate the conformation factor into the model accordingly.

Due to the fact that the tachykinin receptors are membrane-embedded G-protein-coupled receptors consisting of seven transmembrane hydrophobic helical domains and having a large molecular weight, a direct investigation of the conformation adopted by peptides when bound to their native receptors by NMR would be very difficult due to the resulting increase in line broadening, severe overlap of resonances, and the dynamic range problem associated with the high-lipid-concentration vs low-peptide-concentration factor. To compensate for this, micelle systems are often used to mimic a membrane-like environment for NMR studies and in many cases have been shown to induce conformations onto neuropeptides that are considered to be biologically relevant.[15,16]

Applying such a method to the tachykinins, many researchers have extensively studied SP using a variety of membrane mimetic systems in an effort to gain insight into what structural requirements exist for receptor binding.[17−19] On the basis of the results of these studies, a membrane-assisted mechanism for the interactions between peptide neurotransmitters and their receptors has been proposed.[20,21] This mechanism implies that the membrane increases the local concentration of the neuropeptide on the membrane surface. In addition, the process of membrane binding reduces the rotational and translational freedom of the neuropeptide,[22−24] thus facilitating the transition from the usual random coil conformation adopted by neuropeptides in the extracellular solution to a conformation which is recognized by the receptor (i.e., a bioactive conformation).[25−27]

Since it has been shown that membrane mimetic systems are quite capable of inducing structures upon small neuropeptides which may hold some biological relevance,[15−17,28] we have chosen to extend the tachykinin study to include NKA and NKB. If the model holds true, the two neuropeptides should adopt some secondary structure elements which can be correlated to biological activity.

In addition, it would be interesting to determine whether the secondary structure adopted by antagonists selective for the same receptor as the agonists would be similar or different using the same model system. By comparing the structures of both agonists and antagonists, it may be possible to determine information pertaining to the conformational and topographical determinants present in agonist vs antagonist activity at the NK_1 receptor. Therefore, to develop such a comparison, two NK_1 receptor-selective antagonists were studied using the same SDS micelle matrix as NKA and NKB to determine whether the membrane model induces secondary structure characteristics upon the small antagonist ligands that are similar or different to those displayed by agonist ligands. If the structural types of the agonists are indeed different from those of the antagonists, then observations can be made concerning the nature of topographical and conformational determinants for agonist vs antagonist activity in the case of NK_1 receptor-selective ligands.

Here, we present the conformations adopted by four tachykinin analogues in SDS micelles, the two agonists NKA and NKB, as well as the two antagonists [D-Pro^2,D-Phe^7,D-Trp^9]SP and [D-Arg^1,D-Pro^2,D-Phe^7,D-His^9]SP, all of which were investigated by two-dimensional NMR spectroscopy. To our knowledge, this is the first NMR investigation in any solvent system for the two antagonists [D-Pro^2,D-Phe^7,D-Trp^9]SP and [D-Arg^1,D-Pro^2,D-Phe^7,D-His^9]SP as well as the agonist NKB. Our goal is the development of high-quality three-dimensional structures of these peptides in SDS micelle solutions to allow for greater insight into the structural basis for agonist vs antagonist activity at the NK_1 receptor. In addition, it is our goal to obtain information concerning the structural differences within the three NK_1 receptor agonists SP, NKA, and NKB which may aid in explaining the observed binding differences at the NK_1 receptor.

Results

Spectral Assignment: Chemical Shift Assignments. The use of two-dimensional NMR and simulated annealing methods for the determination of solution structures adopted by neuropeptides in the presence of membrane-model systems is well-documented in the literature.[29−31] ^{1}H resonance assignments were determined using the standard two-dimensional NMR sequence-specific resonance assignment techniques of Wüthrich.[32] A WATERGATE−TOCSY[33] experiment was used in each case to identify individual amino acid spin systems by the characteristic coupling patterns of side chains. WATERGATE−NOESY[34] experiments were then used to sequence the spin systems by following the characteristic $C^{\alpha}H-NH$ connectivity pathways. The chemical shift assignments determined for all four peptides using WATERGATE−TOCSY spectra are given in Table 1. A representative WATERGATE−NOESY spectrum showing all assignments for the amide region of NKB is given in Figure 1. WATERGATE−NOESY spectra for the remaining three peptides are available in the Supporting Information.

(A) NKA in SDS-d_{25} Micelles. All amino acids in the primary sequence of NKA are unique, so spin-system assignment was relatively straightforward, with the only difficulty being a minor overlap of the Ser^5 and

Table 1. ^{1}H Chemical Shifts for NKA, NKB, [D-Pro^2,D-Phe^7,D-Trp^9]SP, and [D-Arg^1,D-Pro^2,D-Phe^7,D-His^9]SP

peptide	residue	NH	C$^\alpha$H	C$^\beta$H	others
α-neurokinin	His-1		4.52	3.52, 3.46	8.78 (2H), 7.57 (4H)
	Lys-2	8.77	4.43	1.94, 1.89	1.53, 1.56 (C$^\gamma$H), 1.75, 1.87 (C$^\delta$H), 3.05 (C$^\epsilon$H)
	Thr-3	8.19	4.42	4.27	1.23 (C$^\gamma$H)
	Asp-4	8.31	4.72	2.86	
	Ser-5	8.07	4.38	3.80, 3.77	
	Phe-6	8.07	4.56	3.21, 3.12	7.50 (2,6H), 7.58 (3,5H), 7.60 (1H)
	Val-7	7.66	3.88	2.11	0.97, 0.95 (C$^\gamma$H)
	Gly-8	8.04	3.98, 3.91		
	Leu-9	7.77	4.26	1.83, 1.75	1.64 (C$^\gamma$H), 0.98, 0.92 (C$^\delta$H)
	Met-10	7.80	4.41	2.16, 2.07	2.61, 2.49 (C$^\gamma$H), 2.18 (C$^\epsilon$H)
	term. NH$_2$	7.23, 6.95			
β-neurokinin	Asp-1		4.50	3.16, 3.52	
	Met-2	8.84	4.37	2.19, 2.29	2.65, 2.65 (C$^\gamma$H), 2.27 (C$^\epsilon$H)
	His-3	8.04	4.20	3.08, 3.11	8.69 (2H), 7.33 (4H)
	Asp-4	8.51	4.35	3.36, 3.46	
	Phe-5	8.20	4.44	2.86, 2.88	7.28 (2,6H), 7.35 (3,5H), 7.31 (4H)
	Phe-6	8.03	4.33	2.90, 3.29	7.28 (2,6H), 7.35 (3,5H), 7.31 (4H)
	Val-7	8.04	3.75	2.11	0.95, 0.96 (C$^\gamma$H)
	Gly-8	7.87	3.88		
	Leu-9	7.48	4.15	1.52, 1.61	1.51 (C$^\gamma$H), 0.74, 0.75 (C$^\delta$H)
	Met-10	7.63	4.36	2.14, 2.02	2.60, 2.47 (C$^\gamma$H), 2.05 (C$^\epsilon$H)
	term. NH$_2$	6.32, 7.09			
[D-Pro^2,D-Phe^7,D-Trp^9]SP	Arg-1		4.49	1.55	1.78, 1.90 (C$^\gamma$H), 3.05 (C$^\delta$H), 7.54 (NH$^+$)
	D-Pro-2		4.64	2.25	2.13 (C$^\gamma$H), 3.77 (C$^\delta$H)
	Lys-3	8.36	4.37	1.78, 1.82	1.43, 1.46 (C$^\gamma$H), 1.65 (C$^\delta$H), 4.03 (C$^\epsilon$H)
	Pro-4		4.75	2.19	2.10 (C$^\gamma$H), 3.78, 3.93 (C$^\delta$H)
	Gln-5	8.41	4.24	2.05, 2.06	2.41, 2.43 (C$^\gamma$H), N/A (δNH$_2$)
	Gln-6	8.23	4.35	1.90, 1.99	2.07, 2.19 (C$^\gamma$H), N/A (δNH$_2$)
	D-Phe-7	7.96	4.70	2.96, 2.99	7.28 (2,6H), 7.35 (3,5H), 7.32 (4H)
	Phe-8	7.50	4.65	2.72, 2.96	7.28 (2,6H), 7.35 (3,5H), 7.32 (4H)
	D-Trp-9	8.07	4.33	3.00, 3.14	7.22 (2H), 7.63 (4H), 7.19 (5H), 7.21 (6H), 7.57 (7H), 10.15 (NH)
	Leu-10	7.12	4.07	1.32, 1.45	1.53 (C$^\gamma$H), 0.76 (C$^\delta$H)
	Met-11	7.95	4.37	2.02, 2.18	2.54, 2.60 (CγH), 2.17 (C$^\epsilon$H)
	term. NH$_2$	6.90, 7.56			
[D-Arg^1,D-Pro^2,D-Phe^7,D-His^9]SP	D-Arg-1			1.77, 1.96	N/A (C$^\gamma$H), 3.22 (C$^\delta$H), 7.25 (NH$^+$)
	D-Pro-2		4.38	1.78, 1.97	1.71 (C$^\gamma$H), 3.60 (C$^\delta$H)
	Lys-3	8.12	4.37	2.15	1.56, 1.57 (C$^\gamma$H), 1.84 (C$^\delta$H), N/A (C$^\epsilon$H)
	Pro-4		4.51	2.05, 2.38	1.98 (C$^\gamma$H), 3.17, 3.23 (C$^\delta$H)
	Gln-5	8.31	4.19	1.94	2.36 (C$^\gamma$H), N/A (δNH$_2$)
	Gln-6	8.06	4.32	1.83	2.15 (C$^\gamma$H), N/A (δNH$_2$)
	D-Phe-7	7.73	4.60	2.72	7.29 (2,6H), 7.34 (3,5H), 7.31 (4H)
	Phe-8	7.77	4.52	2.87	7.29 (2,6H), 7.34 (3,5H), 7.31 (4H)
	D-His-9	8.17	4.49	3.18	8.60 (2H), 7.19 (4H)
	Leu-10	8.28	4.19	1.57, 1.74	1.71 (C$^\gamma$H), 0.86 (C$^\delta$H)
	Met-11	7.93	4.41	2.04	2.56 (C$^\gamma$H), 2.20 (C$^\epsilon$H)
	term. NH$_2$	6.89, 7.26			

Phe^6 resonances. Due to this fact, the experiment was performed at 300 K only, with no need to attempt an amide resonance dispersion for increased resolution.

(B) NKB in SDS-d_{25} Micelles. Using the same method, assignments were made for NKB, with an overlap of His^3, Phe^6, and Val^7 being the only difficult assignment. Similar spin systems were distinguished from one another based upon the C$^\alpha$H−NH connectivity pathways. Data were collected at several temperatures, with 315 K yielding the best dispersion of the amide resonances and thus the best resolution.

(C) [D-Pro^2,D-Phe^7,D-Trp^9]SP in SDS-d_{25} Micelles. Assignment was straightforward, with the only problem being an overlap of the D-Phe^7 and Phe^8 connectivities. Minor ambiguities due to the overlap of spectral resonances were resolved by comparison of WATERGATE−NOESY and WATERGATE−TOCSY spectra acquired at different temperatures, with 310 K yielding the best resolution. Verification of the assignments was made by identifying the sequential connectivity pathway linking the C$^\alpha$H of each individual residue with the NH of the residue that follows using a 200-ms NOESY spectrum.

(D) [D-Arg^1,D-Pro^2,D-Phe^7,D-His^9]SP in SDS-d_{25} Micelles. Very little spectral overlap occurred, so assignment was straightforward with no need to attempt to disperse amide resonances by acquiring data at variable temperatures.

Molecular Dynamics and Simulated Annealing: (1) Three-Dimensional Structure. Using the distance restraints shown in Table 2, three-dimensional structures were determined for the four peptides using a molecular dynamics and simulated annealing protocol. A summary of the intraresidue as well as sequential interresidue and medium-range NOEs used as restraints for all four peptides is given in Figure 2. In all cases, 50 structures were generated, with the 25 of lowest energy being used in structural analysis. Statistical data concerning regions of global folding, rmsd values for superimposition, average energies, and distance violations for all four peptides are given in Table 3. Stereoview representations for the four peptides showing backbone superimposition are given in Figure 3. A sequential alignment of the primary structures of the four peptides, denoting sequence homologies as well

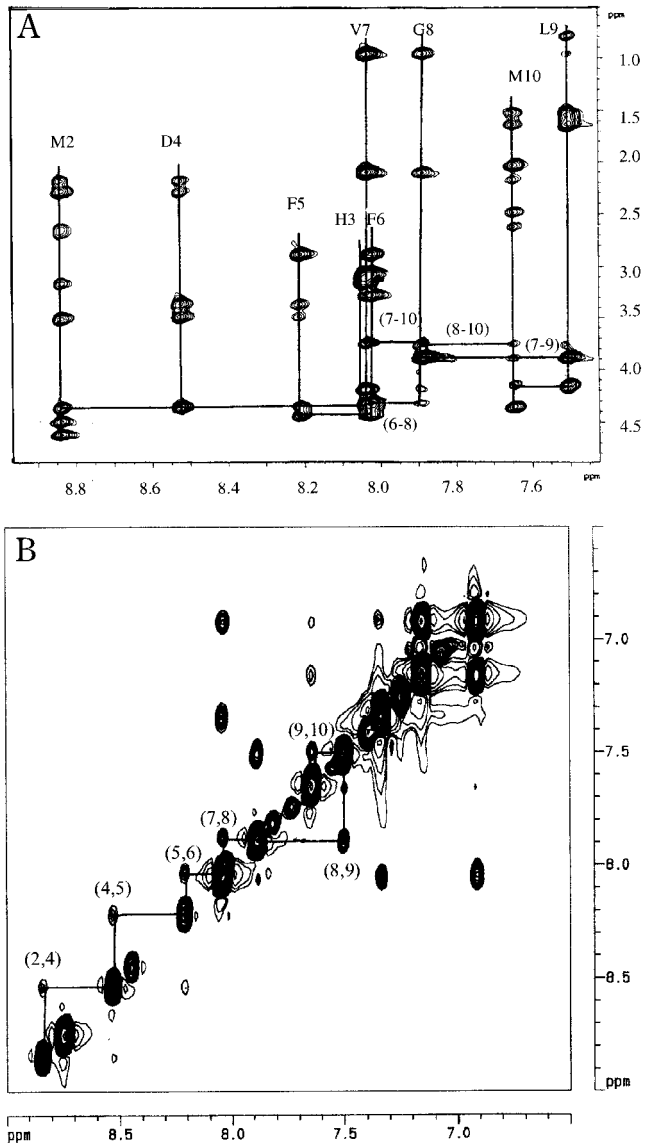

Figure 1. (A) NH−alkyl region and (B) NH−NH region of 600-MHz NOESY spectra for NKB in 50 mM SDS-d_6 micelles, 80% H_2O/20% ^2H_2O at pH = 4.0 and 300 K.

Table 2. Experimental NOEs Used as Restraints in SA Calculations

compound	intra-residual	i to $i+1$	i to $i+2$	i to $i+3$	total
NKA	17	16	5	3	41
NKB	9	12	3	3	27
[D-Pro^2,D-Phe^7,D-Trp^9]SP	8	13	4	0	25
[D-Arg^1,D-Pro^2,D-Phe^7,D-His^9]SP	8	14	4	1	27

as different secondary structure characteristics between the agonists and antagonists, is given in Figure 4.

(A) NKA in SDS-d_{25} Micelles. The presence of several strong NH−NH_{i+1} connectivities, along with C^αH−NH_{i+1}, C^αH−NH_{i+2}, and C^αH−NH_{i+3} connectivities, is sufficient to suggest that some form of helical structure exists. In addition, a weak C^αH−$C^\beta H_{i+2}$ connectivity between residues 6 and 9 stabilizes the helical structure over this region, verifying that a helical structure is the predominant secondary structure for the C-terminal portion of the peptide.

(B) NKB in SDS-d_{25} Micelles. A series of strong NH−NH_{i+1} and C^αH−NH_{i+1} connectivities, along with several overlapping C^αH−NH_{i+2} and C^αH−NH_{i+3} connectivities of medium to weak intensity, suggests that a helical structure should be present throughout most of the peptide.

(C) [D-Pro^2,D-Phe^7,D-Trp^9]SP in SDS-d_{25} Micelles. The presence of a continuous sequence of strong NH−NH_{i+1} and C^αH−NH_{i+1} connectivities, along with overlapping medium to weak C^αH−NH_{i+2} connectivities, is suggestive of a helical structure in the midregion, while a continuous run of weak NH−NH_{i+2} and C^αH−NH_{i+2} connectivities in the C-terminus denotes a β-turn structure in the region consisting of residues 6−9.

(D) [D-Arg^1,D-Pro^2,D-Phe^7,D-His^9]SP in SDS-d_{25} Micelles. The presence of a continuous series of strong NH−NH_{i+1} and C^αH−NH_{i+1} connectivities, along with overlapping weak C^αH−NH_{i+2} and one weak C^αH−$C^\beta H_{i+3}$ connectivity in the midregion, is indicative of a helical structure in the midregion of the peptide, while a continuous run of medium to weak NH−NH_{i+2} and C^αH−NH_{i+2} connectivities in the C-terminus (residues 7−10) indicates that a β-turn exists in this region.

(2) Secondary Structure. The presence and location of peptide secondary structure was estimated using one portion of the chemical shift index (CSI) method of Wishart[35] which estimates certain secondary structure characteristics based on the comparative deviation of the chemical shifts of the C^αH from random coil values for each amino acid. Results for this technique (given in the Supporting Information) indicate structures consistent with the NOE data.

Discussion

High-resolution NMR spectroscopy has been extensively used to determine the possible solution-state conformations of some of the more well-known tachykinin ligands, with results showing that they adopt secondary structure elements in solution environments that are known to promote structure in small peptides (such as micelles and lipids).[17,36−41] We have shown that SDS micelles produce an environment which is an effective matrix for inducing order in the secondary structures of four tachykinin analogues, namely, NKA, NKB, [D-Pro^2,D-Phe^7,D-Trp^9]SP, and [D-Arg^1,D-Pro^2,D-Phe^7,D-His^9]SP.

In a previous study, our group determined that the structure adopted by SP (the primary ligand for the NK_1 receptor) is comprised of a helical midregion with an extended C-terminus when in the presence of 15 mM SDS micelles.[17] Such a structure correlates with that predicted to be biologically active by conformationally restrained analogue studies.[42] In another study, Keire and Fletcher reported a similar structure for SP using 40 mM SDS.[18] In both cases, SP contains a turn structure involving residues 6−9; however, the nature of these turns is different. We reported ϕ and ψ dihedral angles for residues 4−8 of −70 ± 9° and −30 ± 10°, respectively, while Keire and Fletcher reported ϕ and ψ dihedral angles of 30 ± 72° and 16 ± 12° for the same region. There are several possible explanations for the differences in turn geometry. In both studies, the ^{1}H chemical shifts determined were fairly close, with a range of variability of about ±0.1 ppm. However, Keire and Fletcher did not observe any C^αH−NH_{i+2} or C^αH−NH_{i+4} NOEs, whereas we observed three C^αH−NH_{i+2}

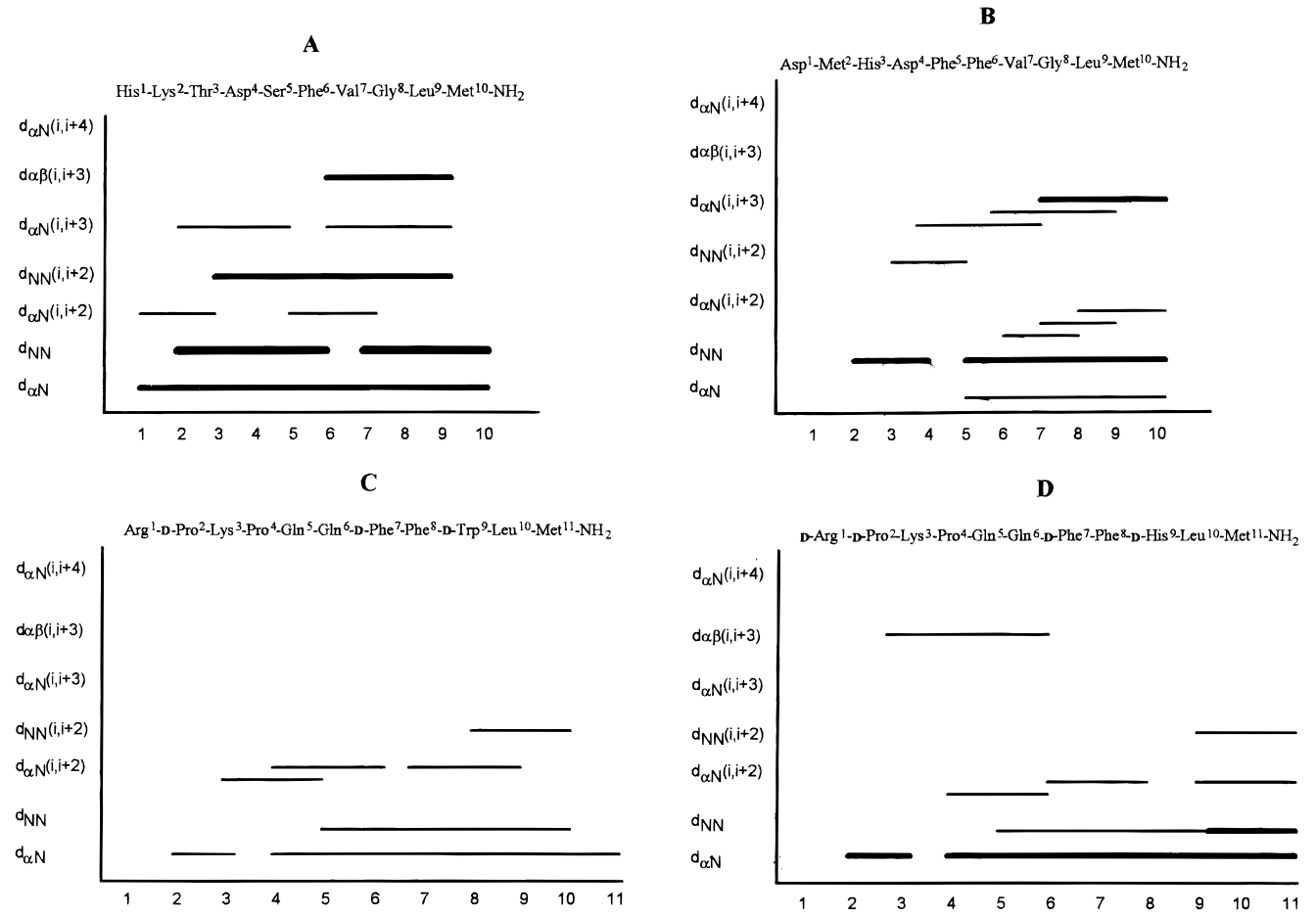

Figure 2. Summary of the sequential and medium-range NOE connectivities observed in (A) NKA in SDS-d_{25} micelles, (B) NKB in SDS-d_{25} micelles, (C) [D-Pro^2,D-Phe^7,D-Trp^9]SP in SDS-d_{25} micelles, and (D) [D-Arg^1,D-Pro^2,D-Phe^7,D-His^9]SP in SDS-d_{25} micelles. Relative NOE intensities are represented by bar thickness.

Table 3. Statistical Data for NKA, NKB, [D-Pro^2,D-Phe^7,D-Trp^9]SP, and [D-Arg^1,D-Pro^2,D-Phe^7,D-His^9]SP

compound	residues	rmsd (Å)	av rmsd (Å)	av energy (kcal)	violations (Å)
NKA	6−10	0.39−1.23	0.84 ± 0.27	227.32 ± 20.2	≤0.175
NKB	4−10	0.09−0.78	0.38 ± 0.27	118.53 ± 29.5	≤0.100
[D-Pro^2,D-Phe^7,D-Trp^9]SP	4−10	0.27−1.12	0.77 ± 0.39	226.69 ± 21.2	≤0.100
[D-Arg^1,D-Pro^2,D-Phe^7,D-His^9]SP	6−10	0.08−0.54	0.38 ± 0.31	175.91 ± 22.9	≤0.100

NOEs and one $C^{\alpha}H-NH_{i+4}$ NOE, all of which are vital for helix formation. Of the remaining $i + 2$ and $i + 3$ NOEs, we observed a total of 16, while Keire and Fletcher only observed 11 (6 of which were common in both studies). Spectra in our study were acquired with a mixing time of 200 ms which allowed for the detection of weaker NOEs, while Keire and Fletcher collected data with a mixing time of 150 ms, possibly accounting for the nonobserved weaker NOEs that were observed by our group. Differences in the solution conditions employed (15 mM SDS, pH = 4.0 (Hicks) vs 40 mM SDS, pH = 5.4, 200 mM NaCl (Keire and Fletcher)) could also explain discrepancies in the structures. However, our structure of SP in 15 mM SDS compared very well to the structure of NKA and NKB determined in 50 mM SDS as shown here, suggesting structure formation independent of micelle concentration above the critical micelle concentration (cmc) for SDS. Finally, our calculations were performed using the modeling package DISCOVER,[43] while Keire and Fletcher used X-PLOR,[44] which may have led to some differences in final structure determination. More recently, Cowsik and coworkers[19] reported structures for SP in DPC micelles that were similar to those determined by our group using SDS. In either case, the structure adopted in both micelle systems correlates with that predicted to be biologically active by conformationally restrained analogue studies, justifying further use of the membrane-model system for conformational studies of small peptides.[42]

In this study, two additional NK_1 receptor-selective agonists (NKA and NKB) were studied using the same membrane-model matrix as the SP study. Results for both show that a helical structure is the predominant secondary structure adopted by the agonists in the presence of the membrane-model system, once again a structure that is consistent with conformationally restrained analogue studies as being biologically active for agonists of the NK_1 receptor. In all three agonists, both the backbone atoms and side chains that make up the midregion of the peptides superimpose very well, indicating that the secondary structure for all three peptides is the same in this region and that the side chains that are similar in hydrophobicity or hydrophi-

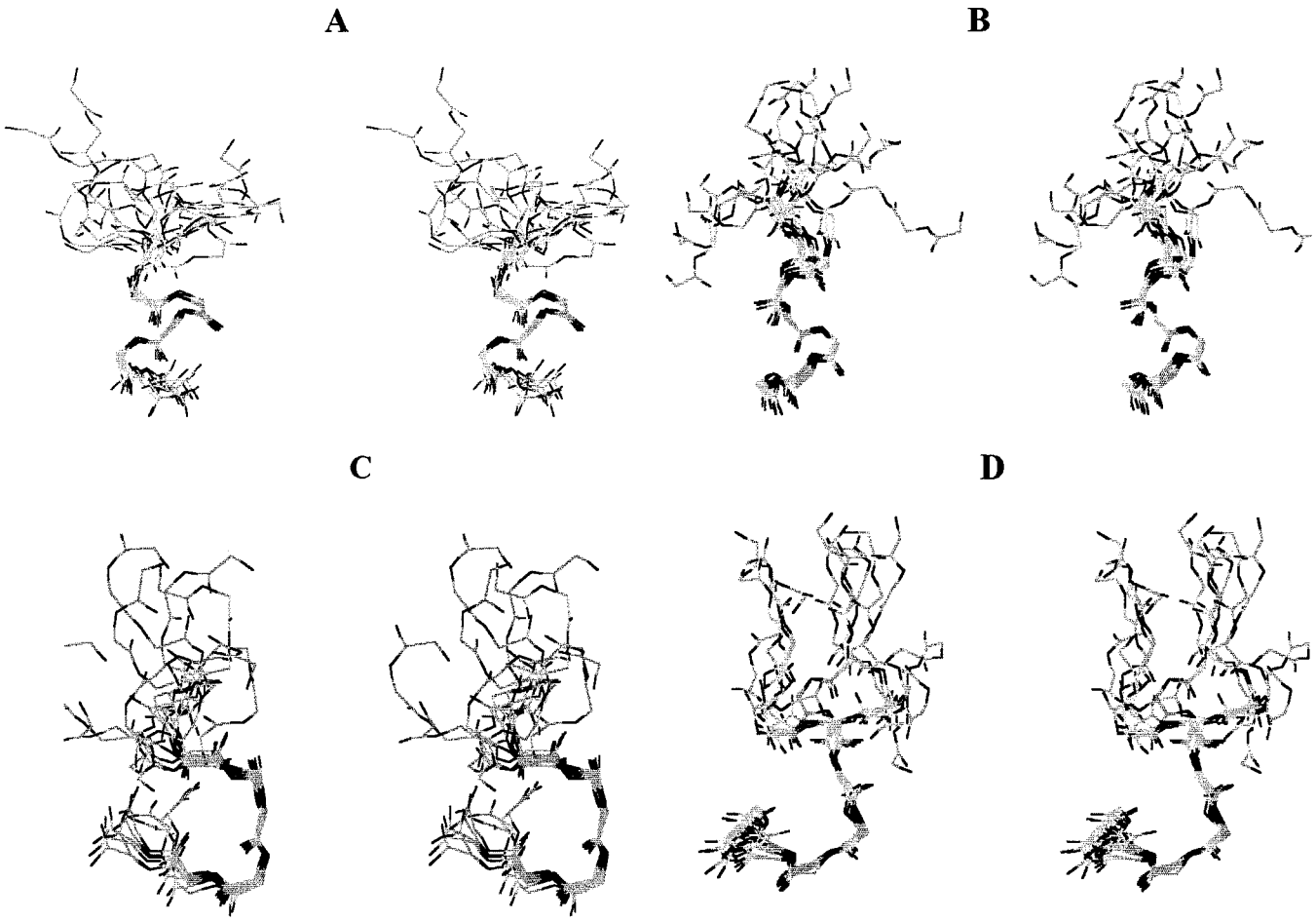

Figure 3. Stereoview superimpositions of the backbone atoms of 25 refined structures of (A) NKA in SDS-d_{25} micelles, (B) NKB in SDS-d_{25} micelles, (C) [D-Pro^2,D-Phe^7,D-Trp^9]SP in SDS-d_{25} micelles, and (D) [D-Arg^1,D-Pro^2,D-Phe^7,D-His^9]SP in SDS-d_{25} micelles.

Compound	Sequence
(A) AGONISTS	
NKA	His^1-Lys^2-Thr^3-Asp^4-*Ser^5-Phe^6-Val^7-Gly^8*-Leu^9-Met^{10}-NH_2
NKB	Asp^1-Met^2-His^3-*Asp^4-Phe^5-Phe^6-Val^7-Gly^8-Leu^9*-Met^{10}-NH_2
(B) ANTAGONISTS	
[**D**-Pro^2,**D**-Phe^7,**D**-Trp^9] SP	Arg^1-**D**-Pro^2-Lys^3-*Pro^4-Gln^5-Gln^6*-**D**-Phe^7-Phe^8-**D**-Trp^9-Leu^{10}-Met^{11}-NH_2
[**D**-Arg^1,**D**-Pro^2,**D**-Phe^7,**D**-His^9]SP	**D**-Arg^1-**D**-Pro^2-Lys^3-*Pro^4-Gln^5-Gln^6*-**D**-Phe^7-Phe^8-**D**-His^9-Leu^{10}-Met^{11}-NH_2

Figure 4. Sequential alignment for (A) NKA in SDS-d_{25} micelles, (B) NKB in SDS-d_{25} micelles, (C) [D-Pro^2,D-Phe^7,D-Trp^9]SP in SDS-d_{25} micelles, and (D) [D-Arg^1,D-Pro^2,D-Phe^7,D-His^9]SP in SDS-d_{25} micelles showing similar structural homologies and different secondary structural characteristics. Regions with helical tendencies are italicized, and regions with turn structures are underlined.

licity occupy the same region of space. Seelig and coworkers have suggested that a possible reason for the helix formation involving the Phe^7 and Phe^8 residues of SP is to provide a hydrophobic face (Phe^7, Phe^8, Leu^{10}) and a hydrophilic face (Gln^6, Gly^9) that will position SP at the receptor binding site in such a fashion as to lead to optimal binding.[45,46] Both NKA and NKB lack the Phe^8 residue, having instead a Val^8 residue which extends the helix length to include Gly^9 in the case of NKA and both Gly^9 and Leu^{10} in the case of NKB (Figure 5). Such a change in helix length alters the position of the hydrophobic and hydrophilic side chains for the C-terminus, decreasing the ability of both ligands to bind as effectively to the NK_1 receptor. Furthermore, stabilization of an increase in helix length results in a reduction in the flexibility of the message region, a situation which has been determined to be unfavorable for receptor binding.[45]

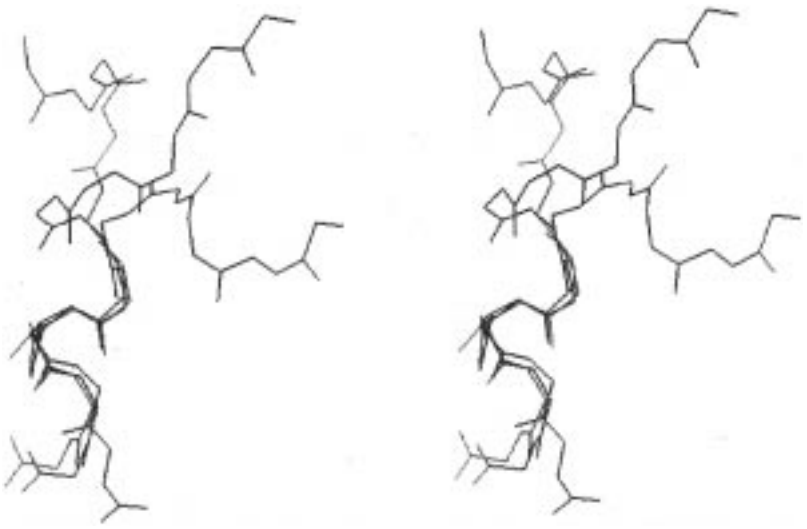

Figure 5. Stereoview of the superimposition of the backbone atoms of SP in SDS-d_{25} micelles (residues 6−9) (magenta), NKA in SDS-d_{25} micelles (residues 5−8) (green), and NKB in SDS-d_{25} micelles (residues 5−8) (blue). The rmsd for the superimposition of NKA onto SP is 0.9047 Å, and the rmsd for the superimposition of NKB onto SP is 0.5705 Å.

Modeling studies conducted by Laoui and co-workers support the assumption that the face of the SP ligand bearing the two Phe residues should interact with the receptor while the three C-terminal residues (Gly-Leu-Met-NH_2) should adopt a more extended conformation.[47] Such a conformation supports the current theory of how SP binds to the NK_1 receptor, in which it has been suggested that the three C-terminal residues (Gly-Leu-Met-NH_2) interact with a transmembrane region of the receptor, while the four N-terminal residues (Arg-Pro-Lys-Pro) interact with an extracellular loop.[48,49] Conventional binding assays have shown that NKA binds to the NK_1 receptor with an affinity roughly equivalent to that of SP; however, NKB exhibits binding approximately 2 orders of magnitude weaker than SP.[50,51] Since the C-terminal composition of both NKA and NKB is identical, it must be the extent of helix formation and the positioning of hydrophobic and hydrophilic side chains (i.e., the conformation) which determine binding efficiency for all three agonists at the NK_1 receptor. Remember: the current model for the binding of SP and other agonists of the NK_1 receptor suggests that the three C-terminal residues (Gly-Leu-Met-NH_2) interact with a transmembrane region of the receptor. Thus, a change in the conformation of the three C-terminal residues will affect receptor binding. For NKA, the helix is extended to include residue 9, and for NKB the helix is extended even further to include residue 10. Seelig suggests that the formation of a stable helical C-terminal segment is, in fact, unfavorable for receptor binding, proven by showing through the use of analogue studies that extending the helix to include residue 9 decreases the degree of binding to the NK_1 receptor.[45] Seelig's observation that a stable helix involving residue 9 is unfavorable for receptor binding supports Convert's proposal that the helix must terminate at residue 8 and that residue 9 must be extended.[42] Note that both NKA and NKB have residue 9 involved in the helix. In light of Seelig's work, the presence of residue 9 in the helix represents a logical rationale for the reduced binding strengths of both neuropeptides at the NK_1 receptor.

In contrast to the NK_1 receptor-selective agonists, the NK_1 receptor-selective antagonists showed a markedly different conformation in the presence of the membrane-model matrix. Maintaining the helical midregion comprised mainly of the Gln^5, Gln^6, and D-Phe^7 residues, the C-terminus adopts a well-defined β-turn in the case of both [D-Pro^2,D-Phe^7,D-Trp^9]SP and [D-Arg^1,D-Pro^2,D-Phe^7,D-His^9]SP, a structure consistent with that believed to be biologically active for NK_1 receptor antagonists based upon conformationally restrained analogue studies.[52] Laoui and co-workers also indicate that the β-turn at the C-terminus is required for antagonist activity.[47] Furthermore, the existence of the helical midregion for both antagonists could explain why both peptides are selective for the NK_1 receptor. The helical midregion could be required for the correct orientation to interact with the second extracellular loop, because Fong and co-workers have determined that the second extracellular loop of the NK_1 receptor aids in the selection of particular ligands based upon amino acid composition as well as three-dimensional conformation.[53] SP, which is helical in the midregion, contains the proper amino acid residues as well as conformation to bind effectively to this region of the receptor. We have already shown that a similar helix exists in other NK_1 receptor agonists. Now, it can also be seen that the helical midregion exists in NK_1 receptor antagonists as well, allowing for the selectivity they show for the NK_1 receptor.

Since all five neuropeptides display a similar helical midregion, yet are known to have different biological activities, one must assume that it is the C-terminal conformation that is responsible for the type of biological activity that is displayed. Comparisons were made between SP and the two NK_1 receptor-selective antagonists to determine what types of differences exist in the C-terminal portion of the peptides. By comparing [D-Arg^1,D-Pro^2,D-Phe^7,D-His^9]SP with SP, it can be seen that the C-termini of the two peptides occupy very different regions of space (Figure 6). In addition, it can also be seen that the C-terminus of the antagonist presents two different faces to the receptor: a hydrophobic face comprised of the Phe^8 and Leu^{10} side chains on one side and a hydrophilic face comprised of the D-His^9 side chain on the other. The importance of this

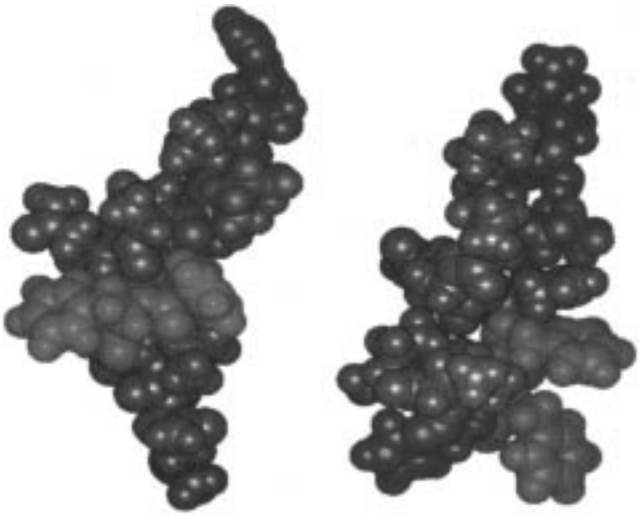

Figure 6. CPK models for (left) SP in SDS-d_{25} micelles and (right) [D-Arg^1,D-Pro^2,D-Phe^7,D-His^9]SP in SDS-d_{25} micelles showing similarities in N-terminal structure and differences in C-terminal structure. Red regions denote positively charged side chains, green regions denote aromatic phenylalanine residues, and gray regions denote side chains that are uncharged.

dual face in the C-terminus on antagonist binding and receptor activation has yet to be determined. Conversely, SP is surrounded on all sides by hydrophobic side chains with a hydrophilic interior. The second antagonist studied also has a β-turn in the C-terminus; however, it does not display a dual-face nature similar to that of [D-Arg^1,D-Pro^2,D-Phe^7,D-His^9]SP. A possible explanation for this is the fact that [D-Pro^2,D-Phe^7,D-Trp^9]SP has been shown through biological assays to exhibit both agonistic and antagonistic properties, a fact which may explain the overall loose nature of the peptide's secondary structure since it may be attempting to adopt both a helical structure and a β-turn structure at the same time, resulting in the loss of a well-defined C-terminal structure.[54] NMR data confirm the fact that some sort of mixture of helical and β-turn families exists, with neither structural type dominating.

Additional comparisons were made between the two NK_1 receptor-selective antagonists and GR-71512, a conformationally restrained peptide known to be an NK_1 receptor antagonist, with the results verifying that the β-turn in the C-terminus is required for antagonistic activity.[52] The backbone atoms of residues 7−11 of the two neuropeptides superimpose onto each other reasonably well, verifying that it is the β-turn in this region that is common to both peptides, thus satisfying a known requirement for biological antagonist activity.

Conclusion

It is impossible to determine at this time whether the structures determined in this study represent the true conformations that these four tachykinin analogues will adopt when bound to the NK_1 receptor. However, it is clear that the results obtained in this study are consistent with proposed biologically active conformations of NK_1 receptor agonists and antagonists. It may simply be a coincidence, but it is interesting to note that the increasing helical content in the conformation of the three C-terminal residues of the agonists and the predictions of helical content by Seelig are consistent with the observed binding order of these compounds to the NK_1 receptor. It is also interesting to note that the structures of the two antagonists indicate a β-turn at the C-terminus. Of further importance is the fact that the fit of the turn can be correlated to the observed biological activity. On the basis of the correlations discussed above, we feel that the conformations adopted by linear tachykinin analogues in the presence of SDS micelles provide valuable information concerning a biologically relevant structure. This structure may be the conformation which is recognized by the receptor, a conformation found at some point during the binding process, a structure very close to the receptor-bound conformation, or some combination of these possibilities. Regardless, these structures can qualitatively be correlated to biological activity and therefore are of great importance in understanding ligand−receptor interactions.

Experimental Section

Materials. NKA, NKB, [D-Pro^2,D-Phe^7,D-Trp^9]SP, [D-Arg^1,D-Pro^2,D-Phe^7,D-His^9]SP, deuterated sodium acetate, and deuterated acetic acid were purchased from Sigma Chemical Co. and used without further purification. Isotopically enriched ^2H_2O was purchased from ISOTEC, Inc. Perdeuterated SDS and 2,2-dimethyl-2-silapentane-5-sulfonate (DSS) were purchased from Cambridge Isotope Co.

Sample Preparation. Samples for all four peptides (NKA, NKB, [D-Pro^2,D-Phe^7,D-Trp^9]SP, [D-Arg^1,D-Pro^2,D-Phe^7,D-His^9]SP) were prepared using 500−700-μL aliquots of a solution composed of 1 mM peptide and 50 mM SDS-d_{25} in 80% H_2O/20% ^2H_2O. All samples were buffered using a sodium acetate buffer (50 mM buffer in the case of NKA; 100 mM buffer for all other peptides) to a pH of 4.0 measured using a Corning model 240 pH meter and are uncorrected for the deuterium isotope effect.

Nuclear Magnetic Resonance. ^{1}H NMR experimental data for NKA, NKB, [D-Pro^2,D-Phe^7,D-Trp^9]SP, and [D-Arg^1,D-Pro^2,D-Phe^7,D-His^9]SP were collected using a Bruker AMX-600 spectrometer. All data for SP were collected using the same instrument and were reported in an earlier study.[17] The 2D pulse sequences used included the WATERGATE−TOCSY[33] with a modified MLEV-17 spin−lock sequence[55] and a 70-ms total mixing time including 2.5-ms trim pulses at both the beginning and the end of the sequence, as well as WATERGATE−NOESY[34] experiments with mixing times of 100, 200, and 300 ms. Spectra for NKA in SDS-d_{25} were collected with 32 transients and 1024 t_1 increments and for NKB, [D-Pro^2,D-Phe^7,D-Trp^9]SP, and [D-Arg^1,D-Pro^2,D-Phe^7,D-His^9]SP in SDS-d_{25} with 128 transients and 1024 t_1 increments, with 1.5-s recycle delays for all experiments. Data were collected at 300 K for NKA, 310 K for [D-Pro^2,D-Phe^7,D-Trp^9]SP and [D-Arg^1,D-Pro^2,D-Phe^7,D-His^9]SP, and 315 K for NKB. The spectral width was 9090.9 Hz in both dimensions, and all spectra were acquired with 2048 data points in F_2. All chemical shifts were referenced internally to DSS (0.00 ppm). Suppression of the H_2O resonance during all NMR data acquisition was achieved by irradiation of the solvent frequency with the aid of a WATERGATE gradient pulse sequence which uses a combination of rf pulses and gradient pulses to remove the unwanted coherence of H_2O.[56] Spectra were processed using UXNMR (Bruker) on an ASPECT X-32 data station. Data were multiplied by a 90° shifted sine−bell window function in each dimension before transformation to produce matrices which consisted of 1024 data points in both dimensions. In certain applications, a trapezoidal window function as well as 2048 × 2048 matrices were used to enhance spectral resolution.

Estimation of Distance and Dihedral Constraints. Data from the three WATERGATE−NOESY experiments conducted for each sample were used to classify peak volumes over a range of strong to very weak corresponding to the upper-

bound interproton distance restraints of 2.7, 3.3, 4.0, and 5.0 Å[57] with strong NOEs (2.7 Å) taken from the 100-ms WATERGATE−NOESY, medium (3.3 Å) from the 200-ms WATERGATE−NOESY, and weak−very weak (4.0 and 5.0 Å) from the 300-ms WATERGATE−NOESY. Since stereospecific assignments could not be made initially, pseudoatoms were employed using the center-of-mass approach, with both intraresidue and long-range correction factors added to the distance restraints. In the case of terminal methyl groups, a distance correction of 0.5 Å was added to the upper limits for distance restraints.[58] After one set of MD/SA calculations, stereospecific assignments were made by manually measuring interproton distances and selecting those which were within the acceptable distance range. Correction factors were removed, and MD/SA calculations were repeated.

Molecular Dynamics and Simulated Annealing. Three-dimensional structures were generated using the experimental NOE distance restraint types shown in Table 2 using the software package DISCOVER (MSI) operating on a Silicon Graphics Iris Crimson workstation. A set of 50 structures was generated for each of the four systems by starting from templates with completely randomized backbone ϕ and ψ torsion angles and extended side chains, followed by the application of a MD/SA protocol similar to that used earlier by our group for work done with SP in SDS-d_{25}.[17]

Acknowledgment. We wish to thank Jason Long and Jason Eakin for their assistance in the laboratory, as well as Reid Bishop for his helpful ideas and constructive criticisms. This research was supported in part by the National Science Foundation EPSCoR Program (Grant EHR 91-08767), NMR facilities, Mississippi Magnetic Resonance Facility, National Science Foundation (Grant CHE-92124521), computer facilities, National Science Foundation (Grant CHE-9205329), and the State of Mississippi and Mississippi State University.

Supporting Information Available: NOESY spectra for NKA, [D-Pro^2,D-Phe^7,D-Trp^9]SP, and [D-Arg^1,D-Pro^2,D-Phe^7,D-His^9]SP and partial CSI analysis for all four peptides (5 pages). Ordering information can be found on any current masthead page.

References

(1) Maggi, C. A. The Mammalian Tachykinin Receptors. *Gen. Pharmacol.* **1995**, *26*, 911−944.
(2) Henry, J. L., Couture, R., Cuello, A. C., Pelletier, G., Quirion, R., Regoli, D., Eds. Discussion of nomenclature for TKs and Tachykinin receptors. In *Substance P and Neurokinins*; Springer-Verlag: New York, 1987.
(3) Gaddum, J. H.; Schild, H. Depressor substances in extracts of intestine. *J. Physiol. London* **1934**, *83*, 1−14.
(4) Von Euler, U. S.; Gaddum, J. H. An Unidentified Depressor Substance in Certain Tissue Extracts. *J. Physiol.* **1931**, *72*, 74.
(5) Kimura, S.; Okada, M.; Sugita, Y.; Kanazawa, I.; Munekata, K. Novel neuropeptides, neuropeptide α and *β*, isolated from porcine spinal cord. *Proc. Jpn. Acad., Ser. B: Phys. Biol. Sci.* **1983**, *59*, 101−104.
(6) Nawa, H.; Hirose, T.; Takashima, H.; Inayama, S.; Nakanishi, S. Nucleotide sequences of cloned cDNAs for two types of bovine brain substance P precursor. *Nature* **1983**, *306*, 32−36.
(7) Hunter, J. C.; Maggio, J. E. Pharmacological characterization of a novel tachykinin isolated from mammalian spinal cord. *Eur. J. Pharmacol.* **1984**, *97*, 159−160.
(8) Tatemoto, K.; Lundberg, J. M.; Jornvall, H.; Mutt, V. Neuropeptide K: isolation, structure and biological activities of a novel brain tachykinin. *Biochem. Biophys. Res. Commun.* **1985**, *128*, 947−953.
(9) Kage, R.; McGregor, G. P.; Thim, L.; Conlon, J. M. Neuropeptide-*γ*: A Peptide Isolated from Rabbit Intestine that is Derived from *γ*-Preprotachykinin. *J. Neurochem.* **1988**, *50*, 1412−1417.
(10) Iversen, L. L.; Watling, K. J.; McKnight, A. T.; Williams, B. J.; Lee, C. M. Multiple Receptors for Substance P and related Tachykinins. In *Topics in Medicinal Chemistry: The Proceedings of the 4th SCI−RSC Medicinal Chemistry Symposium*; 1988; pp 1−9.
(11) Hanley, M. R.; Jackson, T. Substance K Receptor. Return of the magnificent seven. *Nature* **1987**, *329*, 766−767.
(12) Schwyzer, R. Membrane Assisted Molecular Mechanism of Neurokinin Receptor Subtype Selection. *EMBO J.* **1987**, *6*, 2255−2259.
(13) Holzemann, G. *Kontakte (Darmstadt)* **1989**, *2*, 3−12.
(14) Huang, R. R. C.; Vicario, P. P.; Strader, C. D.; Fong, T. M. Identification of Residues Involved in Ligand Binding to the Neurokinin-2 Receptor. *Biochemistry* **1995**, *34*, 10048−10055.
(15) Lee, K. J.; Fitton, J. E.; Wüthrich, K. Nuclear Magnetic Resonance Investigation of the Conformation of Delta-Haemolysin Bound to Dodecylphosphocholine Micelles. *Biochim. Biophys. Acta* **1987**, *911*, 144−153.
(16) Bosch, C.; Brown, L. R.; Wüthrich, K. Physicochemical Characterization of Glucagon-Containing Lipid Micelles. *Biochim. Biophys. Acta* **1980**, *603*, 298−312.
(17) Young, J. K.; Anklin, C.; Hicks, R. P. Nuclear Magnetic Resonance and Molecular Modeling Investigations of the Neuropeptide Substance P in the Presence of 15 mM Sodium Dodecyl Sulfate Micelles. *Biopolymers* **1994**, *34*, 1449−1462.
(18) Keire, D. A.; Fletcher, T. G. The Conformation of Substance P in Lipid Environments. *Biophys. J.* **1996**, *70*, 1716−1721.
(19) Cowsik, S. M.; Lücke, C.; Rüterjans, H. Lipid-induced Conformation of Substance P. *J. Biomol. Struct. Dyn.* **1997**, *15*, 27−35.
(20) Romano, R.; Dufresne, M.; Prost, M. C.; Bali, J. P.; Bayerl, T. M.; Moroder, L. Peptide Hormone-Membrane Interactions. Intervesicular Transfer of Lipophilic Gastrin Derivative to Artificial Membranes and their Bioactivities. *Biochim. Biophys. Acta* **1993**, *1145*, 235−242.
(21) Moroder, L.; Romano, R.; Guba, W.; Mierke, D. F.; Kessler, H.; Delporte, C.; Winand, J.; Christophe, J. New Evidence for a Membrane-Bound Pathway in Hormone Receptor Binding. *Biochemistry* **1993**, *32*, 13551−13559.
(22) Sargent, D. F.; Schwyzer, R. Membrane Lipid Phase as Catalyst for Peptide-Receptor Interactions. *Proc. Natl. Acad. Sci. U.S.A.* **1986**, *83*, 5774−5778.
(23) Schwyzer, R. Estimated Conformation, Orientation, and Accumulation of Dynorphin A-(1−13)-Tridecapeptide on the Surface of Neutral Lipid Membranes. *Biochemistry* **1986**, *25*, 4281−4286.
(24) Schwyzer, R. How Do Peptides Interact with Lipid Membranes and How Does This Affect Their Biological Activity? *Braz. J. Med. Biol. Res.* **1992**, *25*, 1077−1089.
(25) Zetta, L.; De Marco, A.; Bourdenneau, M.; Brevard, C. In *Peptides: Structures and Function. Proceedings of the Ninth American Peptide Symposium*; Deber, C. M., Hruby, V. J., Kopple, K. D., Eds.; Pierce Chemical Co.: Rockford, IL; pp 891−894.
(26) Schwyzer, R. in *Natural Products and Biological Activities*; Imura, H., Goto, T., Murachi, T., Nakajima, T., Eds.; Tokyo Press and Elsevier: Tokyo, 1986; pp 197−207.
(27) Schwyzer, R. Peptide-Membrane Interactions and a New Principle in Quantitative Structure−Activity Relationships. *Biopolymers* **1991**, *31*, 785−792.
(28) Rizo, J.; Blanco, R. J.; Kobe, B.; Bruch, M. D. Conformational Behaviour of *Escherichia coli* OmpA Signal Peptides in Membrane Mimetic Environments. *Biochemistry* **1993**, *32*, 4881.
(29) Ohkubo, H.; Nakanishi, S. Molecular Characterization of the Three Tachykinin Receptors. *Annu. Rev. N. Y. Acad. Sci.* **1991**, *632*, 53.
(30) Convert, O.; Duplaa, H.; Lavielle, S.; Chassaing, G. Influence of the Replacement of Amino Acid by its D-Enantiomer in the Sequence of Substance P. 2. Conformational Analysis by NMR and Energy Calculations. *Neuropeptides* **1991**, *19*, 259−270.
(31) Pellegrini, M.; Mammi, S.; Peggion, E.; Mierke, D. F. Threonine^6-Bradykinin: Structural Characterization in the Presence of Micelles by Nuclear magnetic Resonance and Distance Geometry. *J. Med. Chem.* **1997**, *40*, 92−98.
(32) Wüthrich, K. *NMR of Proteins and Nucleic Acids*; Wiley and Sons: New York, 1986.
(33) Braünschweiler, L.; Ernst, R. R. Coherence Transfer by Isotropic Mixing: Application to Proton Correlation Spectroscopy. *J. Magn. Reson.* **1983**, *53*, 521−528.
(34) Wüthrich, K.; Billeter, M.; Braun, W. Polypeptide Secondary Structure Determination by Nuclear Magnetic Resonance Observation of Short Proton−Proton Distances. *J. Mol. Biol.* **1984**, *180*, 715−740.
(35) Wishart, D. S.; Sykes, B. D.; Richards, F. M. The Chemical Shift Index: A Fast and Simple Method for the Assignment of Protein Secondary Structure through NMR Spectroscopy. *Biochemistry* **1992**, *31*, 1647−1651.
(36) Woolley, G. A.; Deber, C. M. Peptides in Membranes: Lipid-induced Secondary Structure of Substance P. *Biopolymers* **1987**, *26*, 109−121.
(37) Horne, J.; Sadek, M.; Craik, D. J. Determination of the Solution Structure of Neuropeptide K by High-Resolution Nuclear Magnetic Resonance Spectroscopy. *Biochemistry* **1993**, *32*, 7406−7412.

(38) Chassaing, G.; Convert, O.; Lavielle, S. Preferential conformation of substance P in solution. *Eur. J. Biochem*. **1986**, *154*, 77−85.
(39) Wilson, J. C.; Nielsen, K. J.; McLeish, M. J.; Craik, D. J. A Determination of the Solution conformation of the Nonmammalian Tachykinin Eledoisin by NMR and CD Spectroscopy. *Biochemistry* **1994**, *33*, 6802−6811.
(40) Loeuillet, D.; Convert, O.; Lavielle, S.; Chassaing, G. *J. Pept. Protein Res.* **1989**, *33*, 171−180.
(41) Levian-Teitelbaum, D.; Kolodny, N.; Chorev, M.; Selinger, Z.; Gilon, C. 1H NMR Studies of Receptor-Selective Substance P Analogues Reveal Distinct Predominant Conformations in DMSO-d_6. *Biopolymers* **1989**, *28*, 51−64.
(42) Chassaing, G.; Convert, O.; Lavielle, S. In *Peptides 1986, Proceedings of the 19th European Peptide Symposium*; Theoropoulos, D., Ed.; Walter de Gruyter & Co.: Berlin, 1986; pp 301−306.
(43) DISCOVER, MSI Technologies.
(44) X-PLOR, A. Brunger, Yale University.
(45) Seelig, A.; Alt, T.; Lotz, S.; Holzemann, G. Binding of Substance P Agonists to Lipid Membranes and to the Neurokinin-1 Receptor. *Biochemistry* **1996**, *35*, 4365−4374.
(46) Seelig, A.; McDonald, P. M. Binding of the Neuropeptide Substance P to Neutral and Negatively charged Lipids. *Biochemistry* **1989**, *28*, 2940.
(47) Laoui, A.; Luttmann, C.; Morize, I.; Pantel, G.; Morgat, A.; Rubin-Carrez, C.; Laroche, V.; Guitton, J. D.; Gigonzac, O.; James-Surcouf, E. Molecular Mimics as Approaches for Rational Drug Design: Application to Tachykinin Antagonists. In *New Perspectives in Drug Design*; Dean, P. M., Jolles, G., Newton, C. G., Eds.; Academic Press: London, 1995; pp 255−284.
(48) Li, Y. M.; Marnerukia, M.; Stimson, E. R.; Maggio, J. E. Mapping Peptide-binding Domains of the Substance P (NK_1) Receptor from P388D1 Cells with Photolabile Agonists. *J. Biol. Chem*. **1995**, *270*, 1213−1220.
(49) Huang, R. R. C.; Yu, H.; Strader, C. D.; Fong, T. M. Interaction of Substance P with the Second and Seventh Transmembrane Domains of the Neurokinin-1 Receptor. *Biochemistry* **1994**, *33*, 3007−3013.
(50) Mantyh, P. W.; Vigna, G. R.; Maggio, J. E. Receptor Involvement in Pathology and Disease in the Tachykinin Receptors. In *The Tachykinin Receptors*; Buck, S. H., Ed.; Humana Press: Totowa, NJ, 1994; Chapter 18, pp 581−610.
(51) Krause, J. E.; Blount, P.; Sachais, B. S. Molecular Biology of Receptors. In *The Tachykinin Receptors*; Buck, S. H., Ed.; Humana Press: Totowa, NJ, 1994; Chapter 7, pp 165−218.
(52) Ward, P.; Ewan, G. B.; Jordan, C. C.; Ireland, S. J.; Hagan, R. M.; Brown, J. R. Potent and Highly Selective Neurokinin Antagonists. *J. Med. Chem*. **1990**, *33*, 1848−1851.
(53) Fong, T. M.; Yu, H.; Huang, R. R. C.; Strader, C. D. The Extracellular Domain of the Neurokinin-1 Receptor is Required for High Affinity Binding of Peptides. *Biochemistry* **1992**, *31*, 11806−11811.
(54) Peircey, M. F.; Schroeder, L. A.; Folkers, K.; Xu, J.-C.; Horig, J. Sensory and Motor Functions of Spinal Cord Substance P. *Science* **1981**, *214*, 1361−1362.
(55) Bax, A.; Davis, D. G. MLEV-17 Based Two-Dimensional Homonuclear Magnetization Transfer Spectroscopy. *J. Magn. Reson*. **1985**, *65*, 355−360.
(56) Sklenar, V.; Piotto, M.; Leppik, R.; Saudek, V. Gradient-Tailored Water Suppression for 1H-15N HSQC Experiments Optimized to Retain Full Sensitivity. *J. Magn. Reson. Series A* **1993**, *102*, 241−245.
(57) Clore, G. M.; Brunger, A. T.; Karplus, M.; Gronenborn, A. M. Application of Molecular Dynamics with Interproton Distance Restraints to Three-dimensional Protein Structure Determination. A Model Study of Crambin. *J. Mol. Biol*. **1986**, *191*, 523−551.
(58) Wüthrich, K.; Billeter, M.; Braun, W. Psudo-Structures for the 20 common Amino Acids for Use in Studies of Protein conformations by Measurements of Intramolecular Proton−Proton distance constraints with Nuclear magnetic Resonance. *J. Mol. Biol*. **1983**, *169*, 949−961.
(59) Wishart, D.; Sykes, B. *J. Biomol. NMR* **1994**, *4*, 171−180.

JM970789X